Internal friction study of the influence of humidity on set plaster

Malika Saâdaoui, Sylvain Meille, Pascal Reynaud, Gilbert Fantozzi

INTERNAL FRICTION STUDY OF WATER EFFECT ON SET PLASTER

M. Saâdaoui[3], S. Meille[2], P. Reynaud[1*] and G. Fantozzi[1]

[1] GEMPPM, INSA de Lyon, 69621 Villeurbanne, France

[2] Lafarge LCR , B.P. 15, 38 291 St Quentin Fallavier, France

[3] LERSIM, EMI, BP 765, Agdal Rabat, Morocco

Abstract

Internal friction, one of the useful techniques for studying material changes at microscopic level, is used to investigate water effect on mechanical behaviour of set plaster. Internal friction was measured as a function of strain amplitude at different humidity conditions. A weak dependence is observed at low strain amplitude, followed by a steep linear rising above a threshold strain amplitude. Increasing the relative humidity increases the internal friction and lowers the threshold of the rising part. The results provide an experimental evidence of a relative sliding of gypsum crystals enhanced in the presence of water, and a simple viscoelastoplastic rheological model is proposed.

Keywords: Set plaster, Internal friction, water effect.

* Corresponding author

1. Introduction

Set plaster is a common construction material, mainly used for plasterboards for interior partitions. Moreover, due to its low cost and easy shaping, it is often used as a model to study the mechanical behaviour of porous brittle materials. Set Plaster is very sensitive to humidity and it is of importance to understand the mechanisms involved in the presence of water. It has a linear elastic behaviour when it is dry [1, 2] and becomes non-linear and plastic, with relatively high fracture deformation, in the presence of water [1]. Moreover, water absorption results in a drastic deterioration of mechanical properties [3, 4]. Set plaster is also very sensitive to subcritical crack growth [5] and creep at humid environment [6].

Set plaster is made of entangled needle-shaped gypsum crystals with relatively weak interfaces [7] implication of which is important for mechanical behaviour. A recent study on fracture behaviour of set plaster [2] showed that the gypsum needles are often debonded and rarely broken and macroscopic crack propagation occurs by linkage with microcracks issued from weak regions. Coquard et al. [3] attributed the water effect to a decrease of the bonds between gypsum crystals rather to the phenomenon of dissolution–precipitation suggested by Murat et al. [8]. Badens et al. [4] correlated the decrease of Young's modulus of set plaster with increasing humidity to a thickening of adsorbed water layers between gypsum crystals, which allows their sliding.

In this work, Internal friction technique [9], is used to investigate the effect of humidity on set plaster, in order to identify the microstructural mechanisms involved during mechanical behaviour in the presence of water. This method, applied for the first time to plaster, is one of the most useful techniques for studying the changes in materials at microscopic level (diffusive processes, phase transformation, dislocation

motion, grain boundary sliding…) and allows to determine associated energy dissipation.

2. Material and procedure

A set plaster with a porosity of 55% was obtained by hydration of a β hemi-hydrate of 96% purity, at a water/plaster weight ratio of 80%. The ~~set~~ paste was hydrated in saturated conditions during 24 hours and dried at 45°C to evaporate the excess of water trapped in the pores. A network of tangled needles of gypsum characterises the final microstructure, shown in fig. 1.

The internal friction or damping, usually denoted, Q^{-1}, is a measurement of energy dissipation in the material [9]. For a vibrating system, it is proportional to the ratio of the dissipated energy in one cycle, ΔW, to the maximum elastic energy stored in the sample W_{el}. For viscoelastic materials, Q^{-1} is given by:

$$Q^{-1} = \frac{\Delta W}{2\pi W_{el}} = \tan\phi \qquad (1)$$

were ϕ is the loss angle between the applied load and resulting deformation.

In this study, two different techniques were used: a forced torsion pendulum [10] allowing a large variation of the deformation at a low frequency (1Hz), and a bending resonant device [11] working at medium frequency about 1 kHz. Two types of samples, directly moulded, were used for internal friction measurements: rectangular bars (40 x 5 x 1 mm^3) for bending resonant tests and dog-bone specimens, with a central part of 2 x 5 x 2 mm^3 and a total length about 40 mm, for torsion pendulum tests. Confining atmospheres in equilibrium at different partial pressures of water varied the relative

humidity in air, determined with a resolution of 5%. Before the experiments, the samples were maintained 24 h in the testing conditions to ensure their equilibrium.

In the torsion pendulum method, electromagnetic coils applied the shear stress and the strain was measured optically. Special care was paid to sample clamping to minimise experimental artefacts due to sliding or material damage. This has been achieved using a screwed system allowing the adjustment of the clamping force [1]. The internal friction experiments were performed by applying increasing strain amplitudes at ambient temperature (20°C) under a constant frequency of 1 Hz at various humidity conditions:

- dry plaster under low pressure (10^{-2} bar) that allowed to eliminate the water without any dehydration of the gypsum,
- plaster at 35 % and 80% of relative humidity (RH),
- water saturated plaster obtained by wetting the central part of the specimen maintained in equilibrium during 24 hours, to allow the hydration of gypsum.

In the bending resonant bar technique, a rectangular sample was horizontally supported, one side covered with silver paint to make it conducting. Then, a flexural vibration was driven electrostatically at the resonant frequency. The internal friction and Young's modulus were measured at a low deformation of 10^{-6} as a function of the relative humidity.

3. Results and discussion

3.1. Strain dependence of internal friction

The internal friction of set plaster, measured on the torsion pendulum at ambient air (35 % RH), is plotted versus the strain amplitude in fig. 2. It can be seen that a

transition from a weakly damping amplitude dependence to a steep linear dependence occurs at a critical strain amplitude, about 2 $.10^{-3}$. Moreover, the dependence was observed to be reversible, indicating that the energy dissipation mechanism involved, has no important memory effect. This result can be interpreted by analogy with rocks, presenting a similar strain damping dependence [12], the linear part of which is attributed to frictional grain sliding. In the case of set plaster, the internal friction curve suggests an anelastic (?) sliding mechanism at low strains (constant internal friction) and a frictional sliding between the gypsum needle crystals at sufficient large strains.

3.2. Influence of humidity

The influence of the relative humidity (RH) on ~~the~~ damping is shown in fig. 3, where the results corresponding to dry conditions and to a water saturated ~~water~~ plaster~~,~~ are also reported (constant temperature for all the tests 20°C). ~~At~~ In a dry environment, no significant increase of the damping was observed in the range of the applied strain amplitudes. Increasing the relative humidity from 35% (corresponding to ambient air) increases the internal friction and shifts the strain-amplitude-dependent stage to lower strain amplitude. For the water saturated material, the internal friction at low amplitude is 7 times greater than that observed at 35% RH and the rising part is steeper. These results provide an argument for relating water effect to sliding mechanism, enhanced by lubrication due to an increase in water thickness between crystals. The high value of internal friction of water saturated plaster at low strain can be attributed to a decrease of intrinsic surface cohesion of gypsum crystals due to water adsorption. By infiltrating between gypsum crystals, water molecules form a layer that act to shield their interaction, resulting in weaker bonding, compared to that of dry material [3].

To confirm the wetting effect, internal friction was measured on set plaster wetted with ethanol, which spreads on the crystal surfaces without any dissolution–recrystallization mechanism, as gypsum is not soluble in it. The internal friction curve (fig. 4) shows similar strain dependence to that of water saturated plaster, with a lower value of the strain amplitude transition. The shift towards lower level of internal friction for ethanol saturated specimen can be attributed to the influence of the liquid surface energy on the crystal interaction [13]. Due to its larger surface energy, water leads to a larger decrease of the surface energy of plaster resulting in easier sliding.

More precise characterisation of the humidity effect was performed by internal friction and Young's modulus measurements on bending resonant bars at low strain amplitude (10^{-6}). Fig. 5-a, shows a monotonic increase of the internal friction with increasing relative humidity, accompanied by a decrease of the Young's modulus. The results plotted in terms of amount of adsorbed water (fig. 5-b), directly measured by evaluating the weight variation of specimens from dry to wet stabilised state [1] show the importance of the very first adsorbed quantities of water. Internal friction increases steeply during the first 0.1% of water uptake, above which it becomes nearly constant. The same adsorbed amount of water undergoes the total loss of the Young's modulus, which is however, less affected than the internal friction. The relative decrease of E is about 10 %, in agreement with previous studies that had also reported a drastic decrease of the plaster strength for a low relative humidity [3, 4, 14, 15]. The high sensitivity of plaster to humidity is due to the weak interactions involved in its cohesion. The presence of water in very small amounts is sufficient to drastically decrease the crystal bonds. A steep increase of internal friction at a low relative humidity was observed in other porous materials and was linked to H-bonding of water on polar sites [16, 17].

Similar conclusion can be drawn for set plaster, with a distinction between free water and bound water associated with polar sites. The increase of the internal friction reflects the kinetic of adsorption of bound water, responsible of viscoelastic dissipation [16, 18].

3.3. Modeling

The strain dependence of internal friction allows to conclude that energy dissipation is produced by viscoelastic (non-strain-dependent) and plastic (linear strain-dependent) sliding mechanisms. The torsion pendulum results in fig. 3, are described by a simple viscoelastoplastic rheological model (fig. 6), composed with a Maxwell element (stiffness G_1, viscosity η), in series with a slipper (threshold shear stress, τ_0) in parallel with a spring (stiffness G_2). Under torsional strain amplitude γ, the loss angle of the model is given by:

$$\tan\phi = \frac{G_1}{2\pi f\eta} \qquad \text{for } \gamma \leq \frac{\tau_0}{G_1} \qquad \text{(2-a)}$$

$$\tan\phi = \frac{G_1}{2\pi f\eta} + \frac{4G_1}{\pi(G_1+G_2)}\left(\frac{G_1}{\tau_0}\gamma - 1\right) \qquad \text{for } \gamma \geq \frac{\tau_0}{G_1} \qquad \text{(2-b)}$$

where f is the frequency.

The Maxwell element corresponds to the behaviour at low amplitude (constant internal friction) the energy dissipation of which is dictated by the viscosity η. The association of the springs and the sleeper, the threshold of which is correlated to the strain dependence transition, reflects the increase of internal friction at a fixed RH. Using the measured value of the shear modulus G_1 at low strain amplitude, the viscosity, η, and the threshold shear stress, τ_0, were adjusted to the internal friction curves at different humidity conditions (tab 1).

Table 1: Effect of relative humidity on micromechanical parameters

% RH	η (Pa.s)	τ_0 (MPa)
35%	$11.0\ 10^{10}$	6.0
80%	$5.2\ 10^{10}$	5,7
100%	$1.6\ 10^{10}$	4.0

A good agreement can be seen (fig. 7) between the experimental and the theoretical curves corresponding to the model. The decrease of τ_0 and η with increasing humidity (tab. 1) reflects the wetting process, allowing easier sliding at the gypsum crystal interfaces.

The experimental internal friction curves and their closeness to the rheological model provide an evidence of a sliding mechanism enhanced by the weakening of the gypsum crystals bond in the presence of water. The frictional sliding between gypsum crystals, associated with the linear increase of internal friction at high strain, can be correlated to the macroscopic plastic behaviour observed for wet plaster during bending tests [1].

4. Conclusion

Internal friction method was successfully applied to set plaster at different humidity rates and the results are seen as evidence of a sliding mechanism between gypsum crystals, enhanced by water absorption. Internal friction shows a transition from weak strain dependence to a rising linear dependence, corresponding to frictional sliding above a threshold value of the strain amplitude. The results are described in the basis of a viscoelastoplastic model, in agreement with easier relative sliding of crystals when water is adsorbed.

References

1. Meille, S., Correlation between mechanical behavior and microstructure of set plaster, *PhD Thesis, INSA de Lyon, France* 2001.

2. Meille, S., Saâdaoui, M., Reynaud, P. and Fantozzi, G., Mechanisms of rack propagation in dry plaster, *J. Eur. Ceram. Soc.*, 2003, **23**, 3105-3112.

3. Coquard, P. and Boistelle, R., Water and solvent effects on the strength of set plaster. *Int. J. Rock Mech. Min. Sci.*, 1994, **31**, 517-524.

4. Badens, E., Veesler, S., Boistelle, R. and Chatain, D., Relation between Young's modulus of set plaster and complete wetting of grain boundaries by water, *Colloids and surfaces*, 1999, **A 156**, 373 –379.

5. Saâdaoui, M., Reynaud, P. and Fantozzi, G. and Caspar, J.P., Slow crack growth study of plaster using the double torsion method, *Ceram. Inter*, **26**, 2000, 435-439.

6. Sattler, H., Elastic and plastic deformations of plaster units under compressive stress. *Materials and structures*, 1974, **7**, 159-68.

7. Finot, E., Lesniewska, E., Mutin, J.C. and Goudonnet, J.P., Reactivity of gypsum faces according to the relative humidity by scanning force microscopy. *Surface Sci.*, 1997, **384**, 201-217.

8. Murat, M., Pusztaszeri, L., and Gremion, M., Corrélation texture cristalline-propriétés mécaniques de plâtres durcis, *Matériaux et Construction*, 1974, **8**, 377-385.

9. Schaller, R., Fantozzi, G. and Gremaud, G. (ed.), Mechanical spectroscopy Q^{-1}, Ed. trans. Tech. Publications 2001.

10. Etienne, S., Cavaillé, J.Y., Perez, J., Point, R. and Salvia, M., Automatic system for analysis of micromechanical properties. *Rev. Sci. Instrum.*, 1982, **53**, 1261-66.

11. Fantozzi, G., Fouquet, F., Gobin, P.F., Frottement intérieur et anomalie de module de l'aluminium irradié et déformé à basse température. *Mémoires Scientifiques de la Revue de Métallurgie*, 1972, **69**, 641-652.

12. Mavko, G., Frictional attenuation: an inherent amplitude dependence. *J. Geophys Res.*, 1979, **84**, 4769-75.

13. Kato, Y., Matsui, M. and Umeya, K., Influence of surface energy on the mechanical properties of hardened gypsum, *Gypsum and lime*, 1980, 166, 3-9.

14. Andrews, H., The effect of water contents on the strength of calcium sulfate plaster products. *J. Soc. Chem. Indus.*, 1946, **5**, 125-28.

15. Chappuis, J., A model for a better understanding of the cohesion of hardened hydraulic materials. *Colloids and Surfaces* , 1999, **A 156**, 223-241

16. Lepage, J., On the mechanosorptive effect in porous ceramics Part I: Experimental results, *J. mater. Sci.* 2001, **36**, 3963-71.

17. Lepage, J., On the mechanosorptive effect in porous ceramics Part II: Effect of heating on alumina, *J. mater. Sci.* 2002, **37**, 3405-13.

18. Tittmann, B.R., Clark, V.A., Richardson, J.M. and Spencer, T.W., Possible mechanism for seismic attenuation in rocks containing small amounts of volatiles, *J. of Geophys. Res.,* 1980, **85**, 5199-5208.

Figures

Figure 1: SEM micrograph showing the microstructure of set plaster.

Figure 2: Internal friction of set plaster, measured on the torsion pendulum at ambient air, versus strain amplitude.

Figure 3: Internal friction versus strain amplitude at different conditions of humidity.

Figure 4: Comparison of internal friction for ethanol and water saturated plaster.

Figure 5: Internal friction and Young's modulus, obtained at low strain amplitude (10^{-6}) on resonant flexural bars, as a function of relative humidity (a) and as a function of the amount of adsorbed water (b). Each experimental value corresponds to a stabilised state.

Figure 6: Viscoelastiplastic model proposed to describe the internal friction of set plaster.

Figure 7: Comparison of the experimental internal friction curves obtained at different humidity conditions (symbols) with theoretical curves (lines) corresponding to the model.

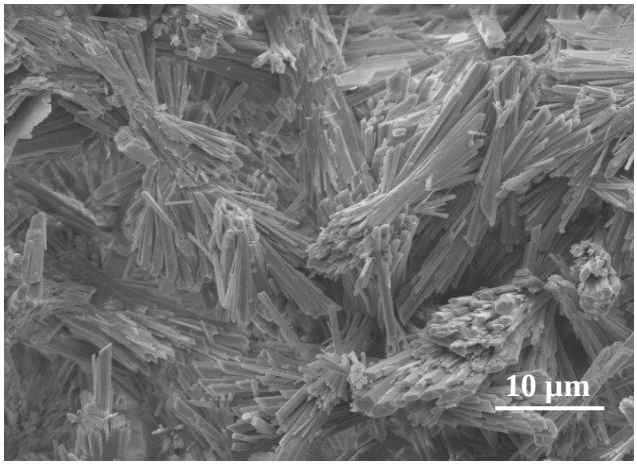

Figure 1

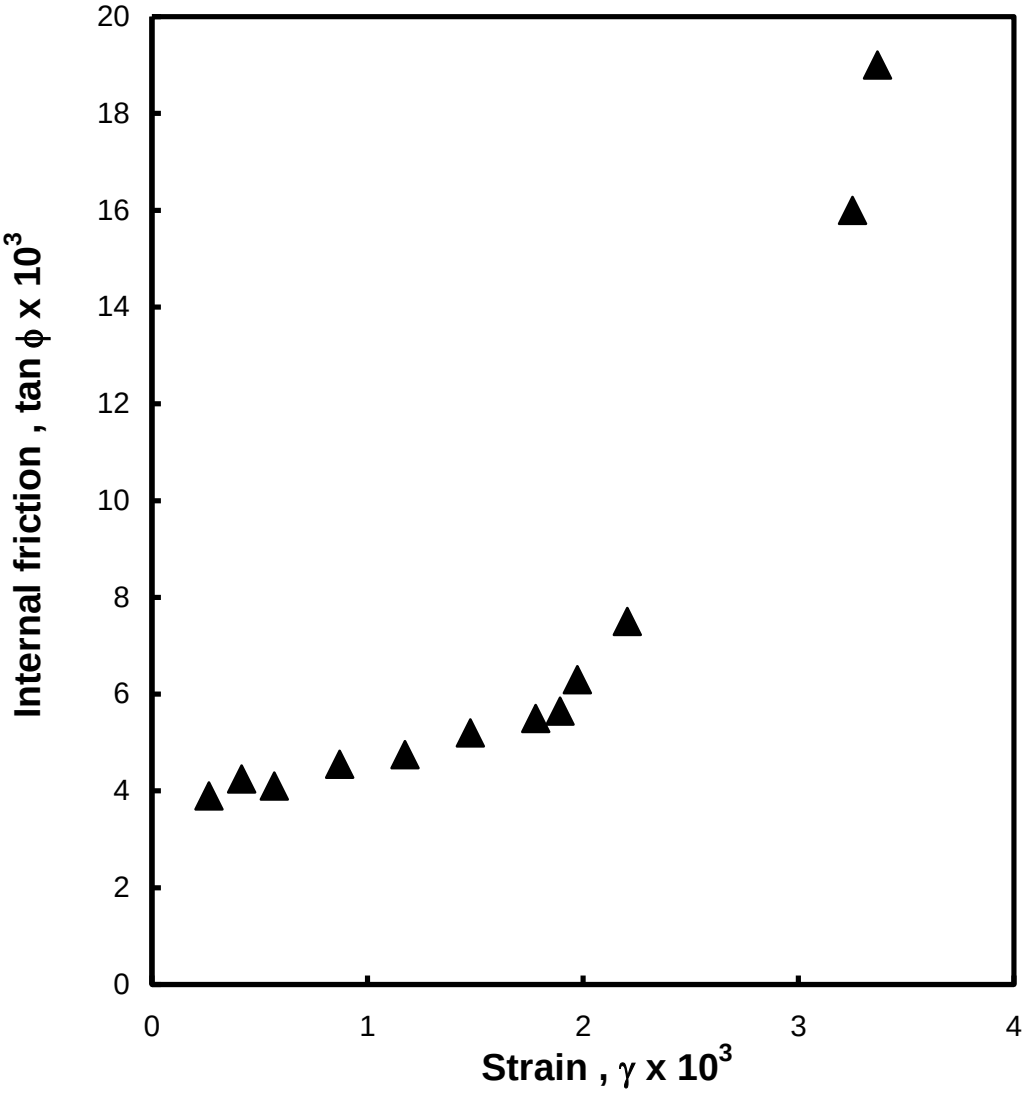
Internal friction , tan ϕ x 10^3
Strain , γ x 10^3
0
2
4
6
8
10
12
14
16
18
20
0
1
2
3
4

Figure 2

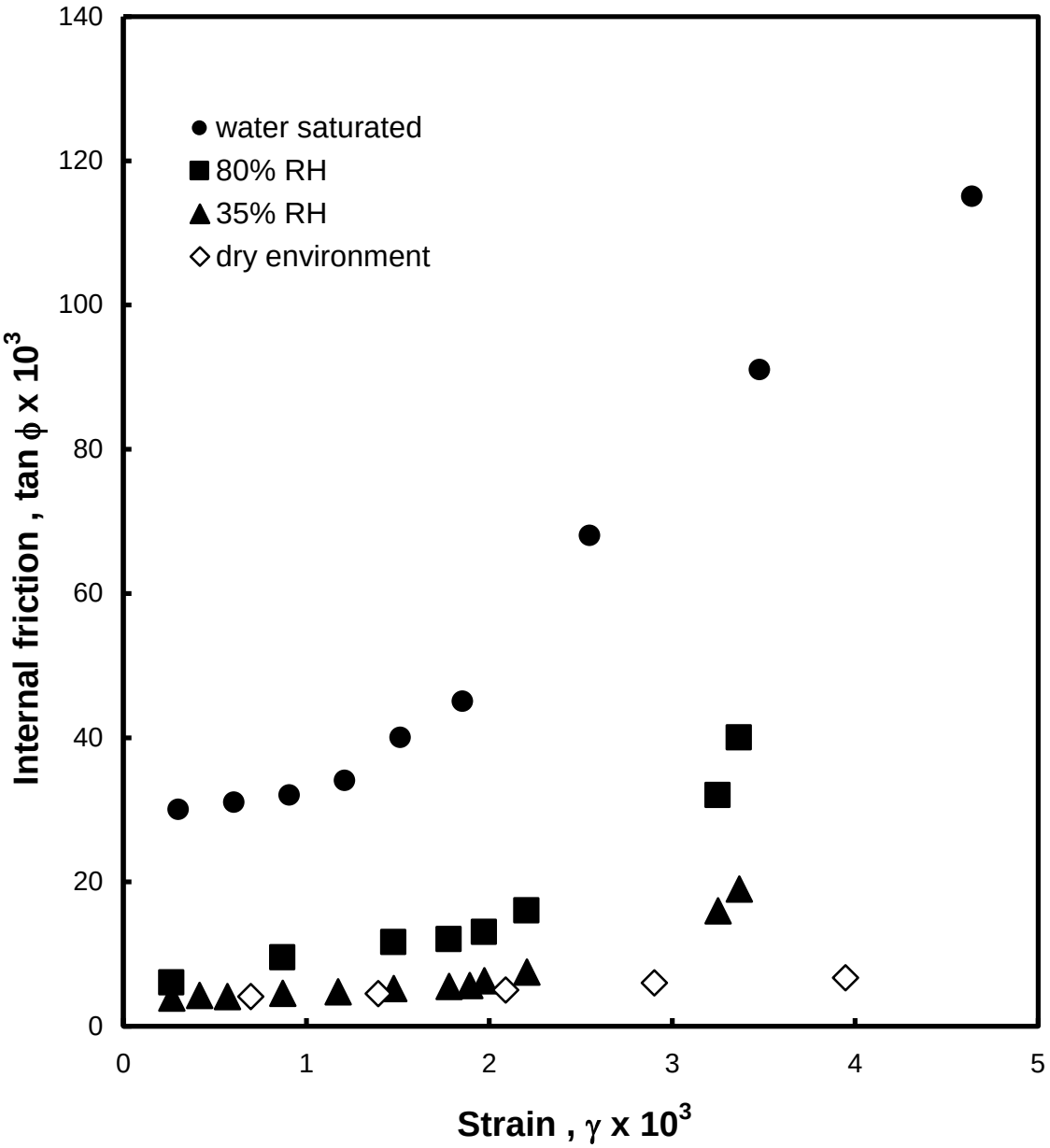
water saturated
80% RH
35% RH
dry environment
Internal friction , tan ϕ x 10^3
Strain , γ x 10^3
0
20
40
60
80
100
120
140
0
1
2
3
4
5

Figure 3

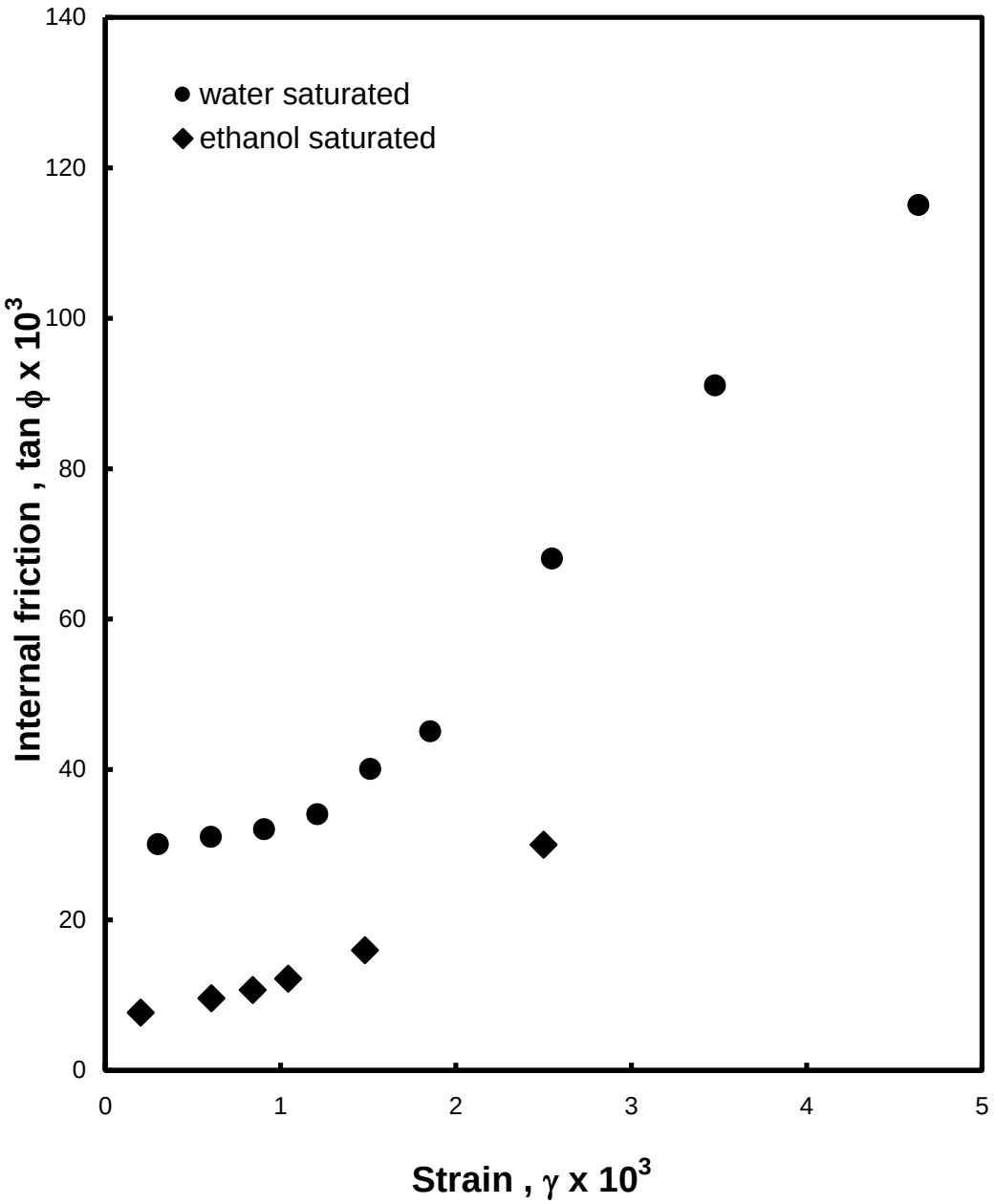
water saturated
ethanol saturated
Internal friction , tan ϕ x 10^3
Strain , γ x 10^3
0
20
40
60
80
100
120
140
0
1
2
3
4
5

Figure 4

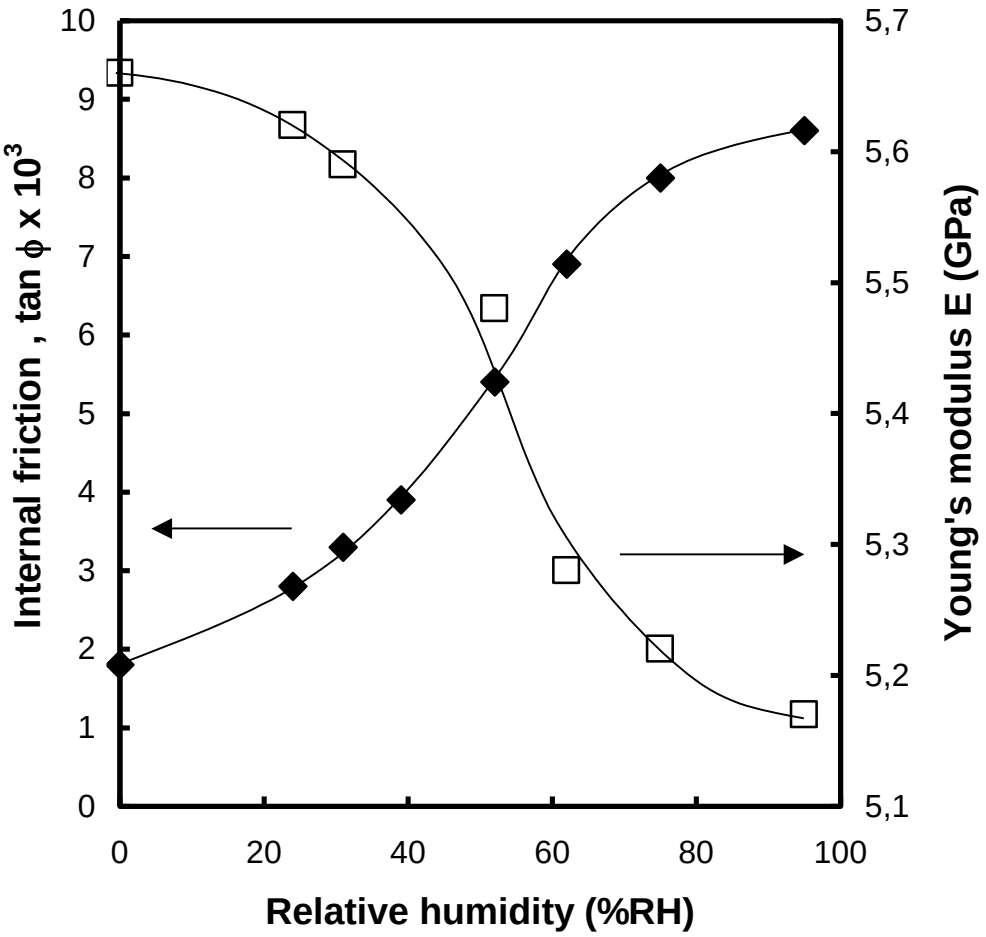
Internal friction , tan ϕ x 10³
Young's modulus E (GPa)
Relative humidity (%RH)
0
1
2
3
4
5
6
7
8
9
10
5,1
5,2
5,3
5,4
5,5
5,6
5,7
0
20
40
60
80
100

Figure 5a

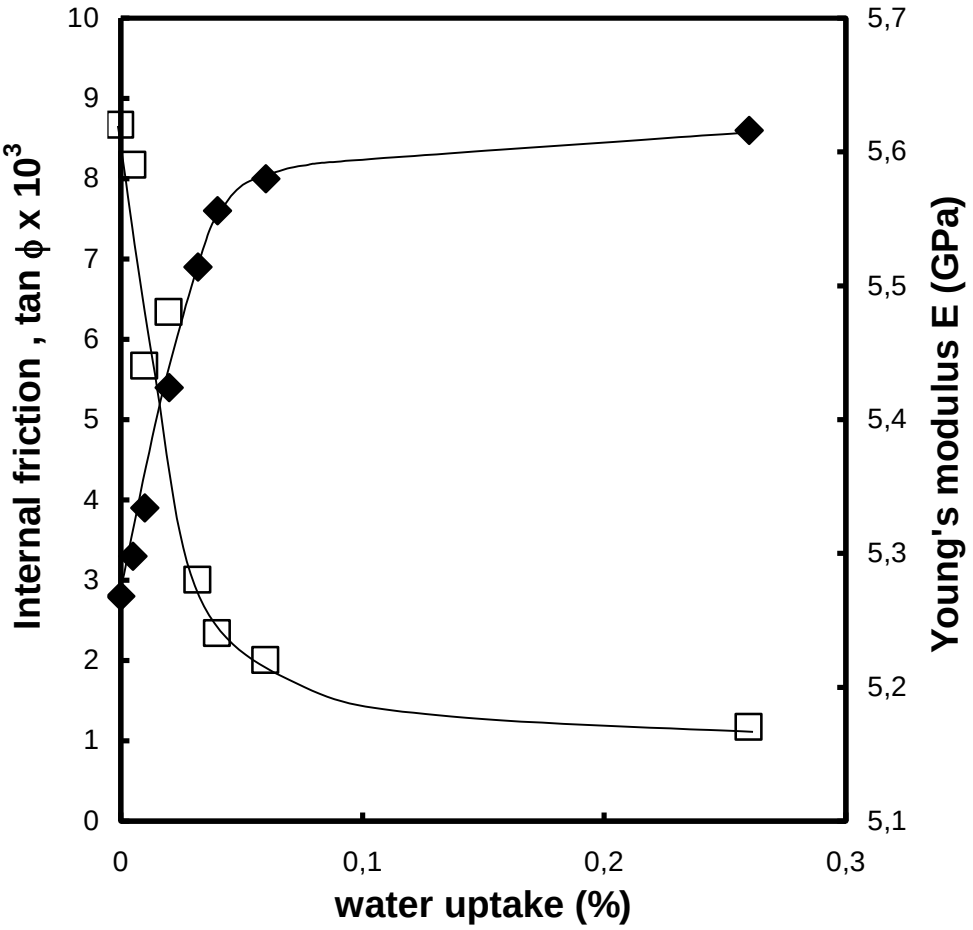
Internal friction , tan ϕ x 10³
Young's modulus E (GPa)
water uptake (%)
10
9
8
7
6
5
4
3
2
1
0
5,7
5,6
5,5
5,4
5,3
5,2
5,1
0
0,1
0,2
0,3

Figure 5b

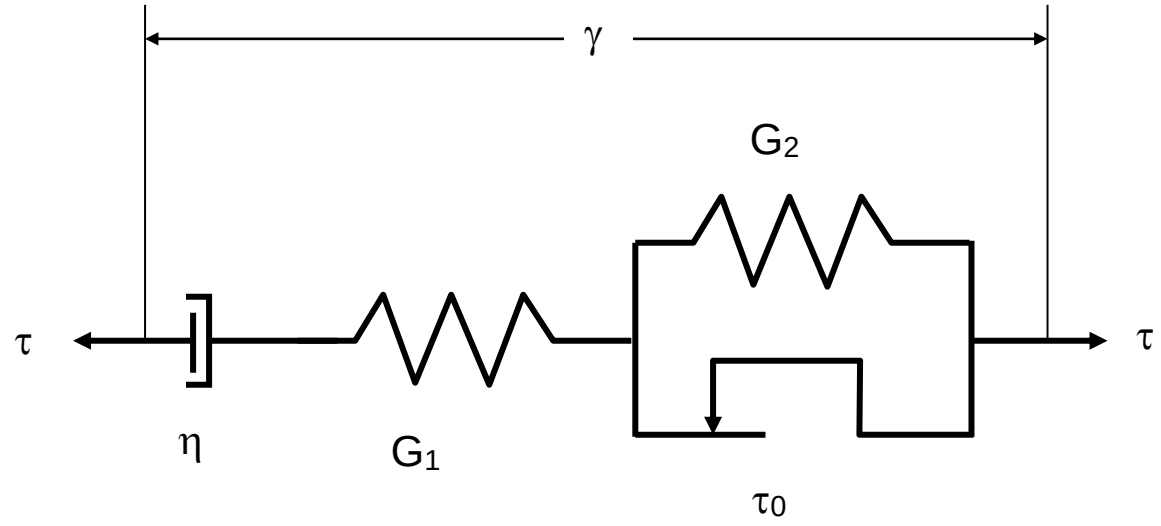

Figure 6

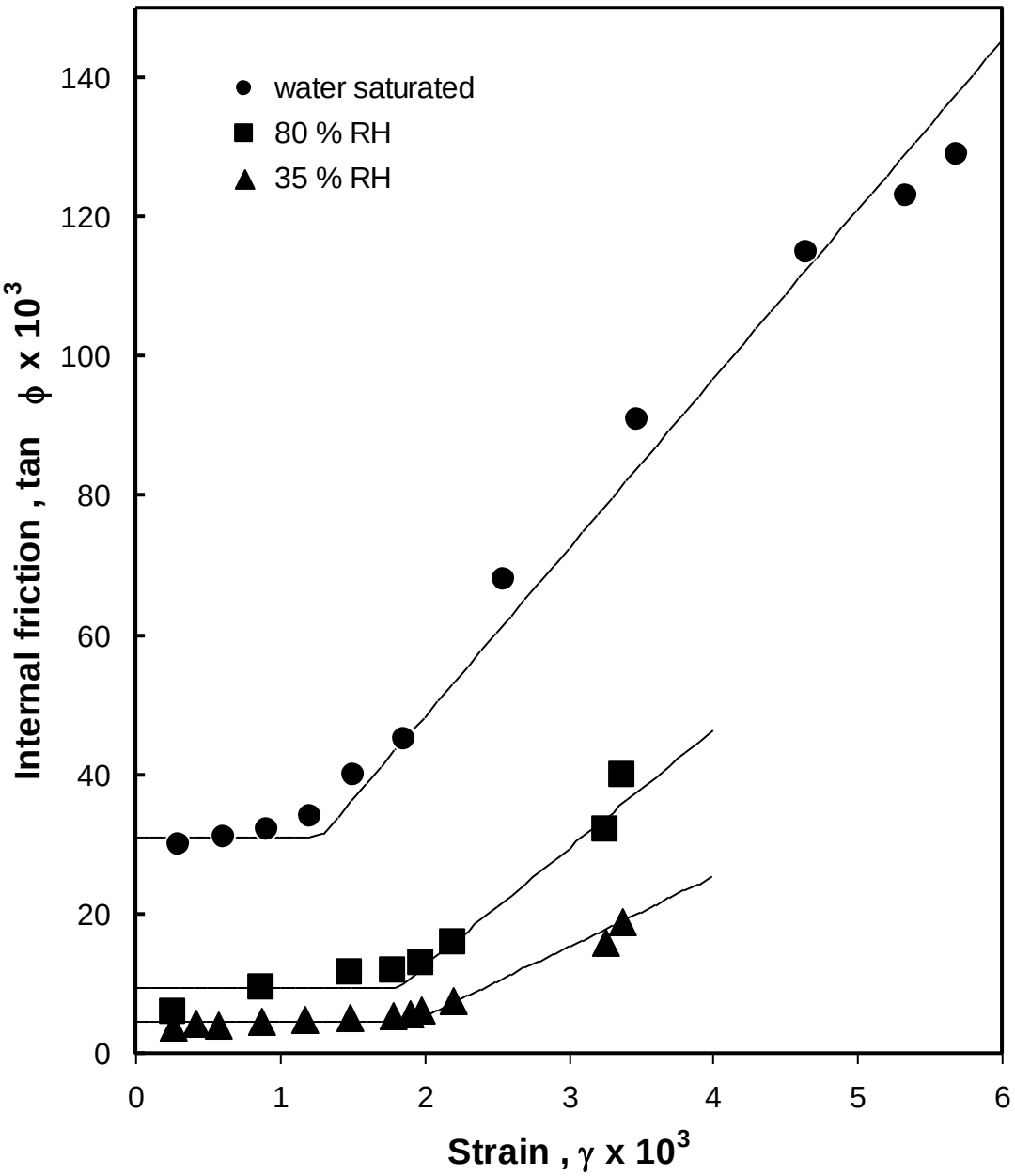
water saturated
80 % RH
35 % RH
Internal friction , tan ϕ x 10^3
Strain , γ x 10^3
0
20
40
60
80
100
120
140
0
1
2
3
4
5
6

Figure 7

% RH	**η (Pa.s)**	**τ_0 (MPa)**
35%	$11.0\ 10^{10}$	6.0
80%	$5.2\ 10^{10}$	5,7
100%	$1.6\ 10^{10}$	4.0

Table 1